Discovery of 1-[3-(Aminomethyl)phenyl]-*N*-[3-fluoro-2′-(methylsulfonyl)-[1,1′-biphenyl]-4-yl]-3-(trifluoromethyl)-1*H*-pyrazole-5-carboxamide (DPC423), a Highly Potent, Selective, and Orally Bioavailable Inhibitor of Blood Coagulation Factor Xa[1]

Donald J. P. Pinto,* Michael J. Orwat, Shuaige Wang, John M. Fevig, Mimi L. Quan, Eugene Amparo, Joseph Cacciola, Karen A. Rossi, Richard S. Alexander, Angela M. Smallwood, Joseph M. Luettgen, Li Liang, Bruce J. Aungst, Matthew R. Wright, Robert M. Knabb, Pancras C. Wong, Ruth R. Wexler, and Patrick Y. S. Lam

DuPont Pharmaceuticals Company, Experimental Station, P.O. Box 80500, Wilmington, Delaware 19880-0500

Received September 19, 2000

Factor Xa (fXa) plays a critical role in the coagulation cascade, serving as the point of convergence of the intrinsic and extrinsic pathways. Together with nonenzymatic cofactor Va and Ca^{2+} on the phospholipid surface of platelets or endothelial cells, factor Xa forms the prothrombinase complex, which is responsible for the proteolysis of prothrombin to catalytically active thrombin. Thrombin, in turn, catalyzes the cleavage of fibrinogen to fibrin, thus initiating a process that ultimately leads to clot formation. Recently, we reported on a series of isoxazoline and isoxazole monobasic noncovalent inhibitors of factor Xa which show good potency in animal models of thrombosis. In this paper, we wish to report on the optimization of the heterocyclic core, which ultimately led to the discovery of a novel pyrazole SN429 (**2b**; fXa $K_i = 13$ pM). We also report on our efforts to improve the oral bioavailability and pharmacokinetic profile of this series while maintaining subnanomolar potency and in vitro selectivity. This was achieved by replacing the highly basic benzamidine P_1 with a less basic benzylamine moiety. Further optimization of the pyrazole core substitution and the biphenyl P_4 culminated in the discovery of DPC423 (**17h**), a highly potent, selective, and orally active factor Xa inhibitor which was chosen for clinical development.

Introduction

Anticoagulants currently available for the treatment and prevention of thromboembolic diseases include warfarin (Coumadin), heparins, hirudin, hirulog, and argatroban.[2−7] Coumadin, a vitamin K-dependent inhibitor, has a slow onset, high oral efficacy, and long duration of action. Heparins and direct thrombin inhibitors have a rapid onset of action, but they must be administered parenterally. The normal protocol for patients on these therapies requires careful monitoring of clotting times to achieve efficacy and dose titration to minimize excessive bleeding.[5] Therefore, there is a serious effort to identify orally active anticoagulants that are clinically safe and which require less monitoring.

Factor Xa (fXa), a trypsin-like serine protease, holds the central position that links the intrinsic and extrinsic mechanisms in the blood coagulation cascade.[8] The physiological role of activated fXa is to proteolytically activate thrombin.[9] Thrombin has several procoagulant functions that include the activation of platelets, the feedback activation of other coagulation factors, and the conversion of fibrinogen to insoluble fibrin clots. Small molecule thrombin inhibitors have been intensely investigated.[10] More recently, direct inhibition of fXa has emerged as an attractive strategy for the discovery of novel antithrombotic agents.[10,11] Since fXa inhibitors

specifically affect coagulation, but not platelet function, this mechanism may be anticipated to have less potential to increase the risk of abnormal bleeding relative to thrombin inhibitors and antiplatelet agents. A comparison between hirudin (a thrombin inhibitor) and tick anticoagulant peptide (TAP, an fXa inhibitor) suggests that inhibition of fXa may result in less bleeding risk, leading to a more favorable safety/efficacy ratio.[12]

Several potent monobasic inhibitors of fXa have been published (from our laboratories as well as by others).[13] Our efforts have recently led to the discovery of potent isoxazoline analogues such as SF303[14] and, more recently, include potent isoxazoles such as SA862 (**1**, fXa $K_i = 0.15$ nM, Figure 1).[15] The lack of chirality of the isoxazole and its high affinity for fXa made it an attractive template for further optimization. In this paper, we wish to discuss the SAR of other five-membered heterocyclic templates in which the point of attachment to the P1 substituent is through a nitrogen atom on the heterocycle.

Chemistry

The synthesis of the 3-unsubstituted pyrazole **2a**, a compound chosen to best mimic the isoxazole core, was accomplished quite readily starting with the condensation of 3-cyanophenylhydrazine and 4-(dimethylamino)-2-oxo-but-3-enoic acid ethyl ester in acetic acid (Scheme 1).[16] The condensation afforded a 1:1 regioisomeric mixture of 3- and 5-substituted pyrazole esters. The desired pyrazole ester **4a** was obtained following puri-

* Corresponding author. E-mail address: Donald.J.Pinto@dupontpharma.com. Phone: (302)695-1429. Fax: (302)695-1502.
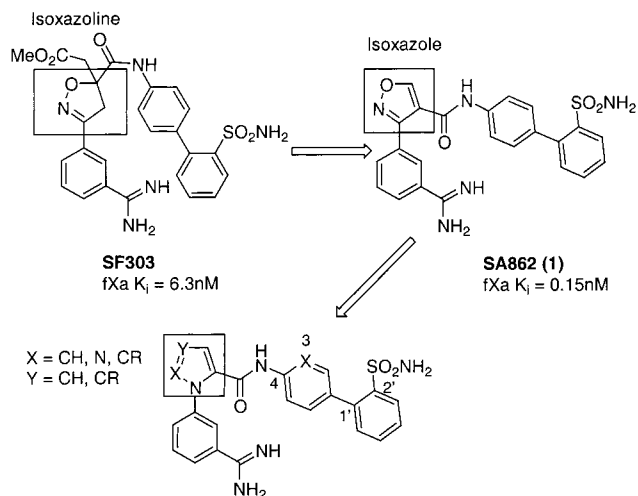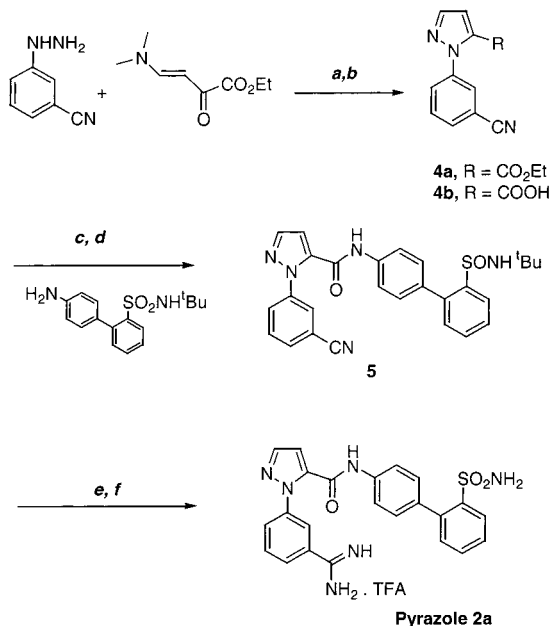
Figure 1. Optimization of the five-membered heterocyclic template.

Scheme 1. Synthesis of Pyrazole **2a**[a]

[a] (**a**) AcOH reflux, 17%; (**b**) LiOH/THF/water, 98%; (**c**) oxalyl chloride/CH$_2$Cl$_2$; (**d**) DMAP/CH$_2$Cl$_2$, 76%; (**e**) HCl, MeOH; (**f**) ammonia/MeOH, 45%.

fication via flash chromatography. Hydrolysis of the ester under basic conditions (LiOH/THF/water) gave the requisite pyrazole carboxylic acid derivative **4b**, which was treated with oxalyl chloride to form the acid chloride. This was then coupled with 4′-amino[1,1′-biphenyl]-2-*tert*-butylsulfonamide[14a] to provide the key intermediate **5**. Treatment of **5** under the Pinner conditions[14,15] (HCl/MeOH) afforded the imidate which was immediately reacted with excess ammonia in methanol to afford pyrazole analogue **2a** in moderate yield. The *tert*-butylsulfonamide substituent is simultaneously deprotected to the primary sulfonamide under these conditions.

The synthesis of a 3-substituted pyrazole **2b** is outlined in Scheme 2. Condensation of 3-cyanophenyl-hydrazine with methyl 2-methoxyimino-4-oxopentanoate afforded pyrazole **6** regioselectively.[17] Hydrolysis of **6** under basic conditions (LiOH/THF/water) gave the requisite carboxylic acid **6a** in good yield. This was then

Scheme 2. Synthesis of 3-Methyl Pyrazole Analogue **2b**[a]
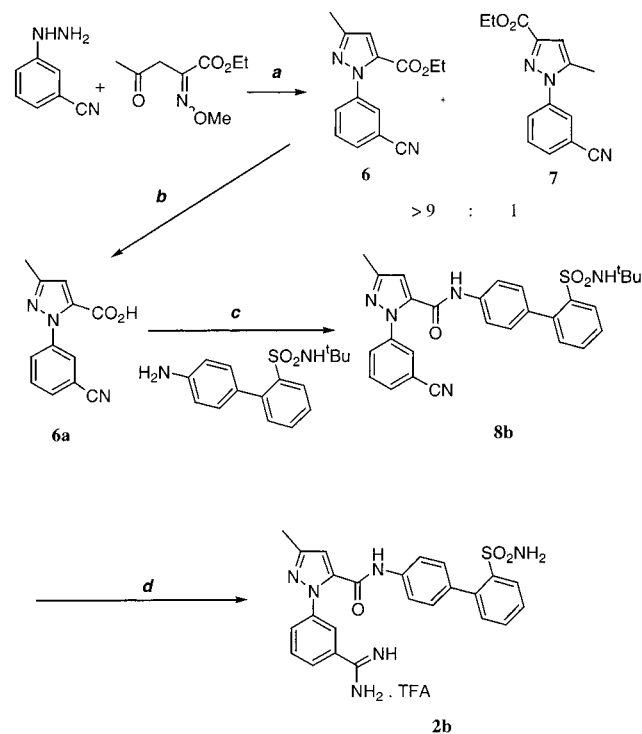
[a] (**a**) Acetic acid reflux, 75%, separated via flash chromatography; (**b**) LiOH/THF/H$_2$O, 90%; (**c**) oxalyl chloride/CH$_2$Cl$_2$ rt; DMAP/CH$_2$Cl$_2$/rt, 99%; (**d**) HCl/MeOH/ammonium carbonate/MeOH, TFA 80 °C, 36%.

coupled to 4′-amino[1,1′-biphenyl]-2-*tert*-butylsulfon-amide via the intermediate acid chloride (oxalyl chloride/DMAP, dichloromethane) to afford **8**. Alternatively, the ester **6** can be coupled with 4′-amino[1,1′-biphenyl]-2-*tert*-butylsulfonamide using the Weinreb trimethyl-aluminum[18] methodology to afford intermediate **8b** in good yield. Most of the amide P$_4$ variants, the 3-*n*-butyl analogue **2c**, and the *N*-methylated amide analogue **2d** were also prepared via the methodology outlined for **2b**. The desired benzamidine pyrazole analogues **2b**−**n** were obtained from the corresponding benzonitrile precursors via the Pinner amidine protocol described previously.

The synthesis of the trifluoromethylpyrazole analogue **14a** is outlined in Scheme 3. Condensation of *m*-bromo-phenylhydrazine with commercially available 1,1,1-trifluoro-2,4-pentanedione (Aldrich) afforded an insepa-rable regioisomeric mixture (8:2) of pyrazoles **9a** and **9b**. Treatment of **9a** and **9b** with copper cyanide in *N*-methyl pyrrolidinone at reflux provided cyanophenyl pyrazole intermediates **10a** and **10b**. Treatment of this mixture with NBS in refluxing carbon tetrachloride afforded the alkylhalides which were immediately con-verted to the hydroxymethyl intermediates **11a** and **11b** under basic conditions. At this stage the desired pyr-azole intermediate **11a** was easily separated and puri-fied via flash chromatography. Oxidation of **11a** with a mixture of ruthenium trichloride and sodium periodate then afforded the desired 3-trifluoromethylpyrazole-5-carboxylic acid intermediate **12**. Acid chloride coupling of **12** to 4′-amino[1,1′-biphenyl]-2-*tert*-butylsulfonamide provided benzonitrile precursor **13a**, which was treated under the Pinner amidine protocol to afford the desired benzamidine analogue **14a**. Trifluoromethylpyrazole analogues **14b**−**f** were prepared in a similar manner.

Scheme 3. Synthesis of 3-Trifluoromethylpyrazole Analogue **14a**

8 : 2
9a **9b** **10a** **10b**

11a

+

11b

12

13a

X, Y = CH

14a
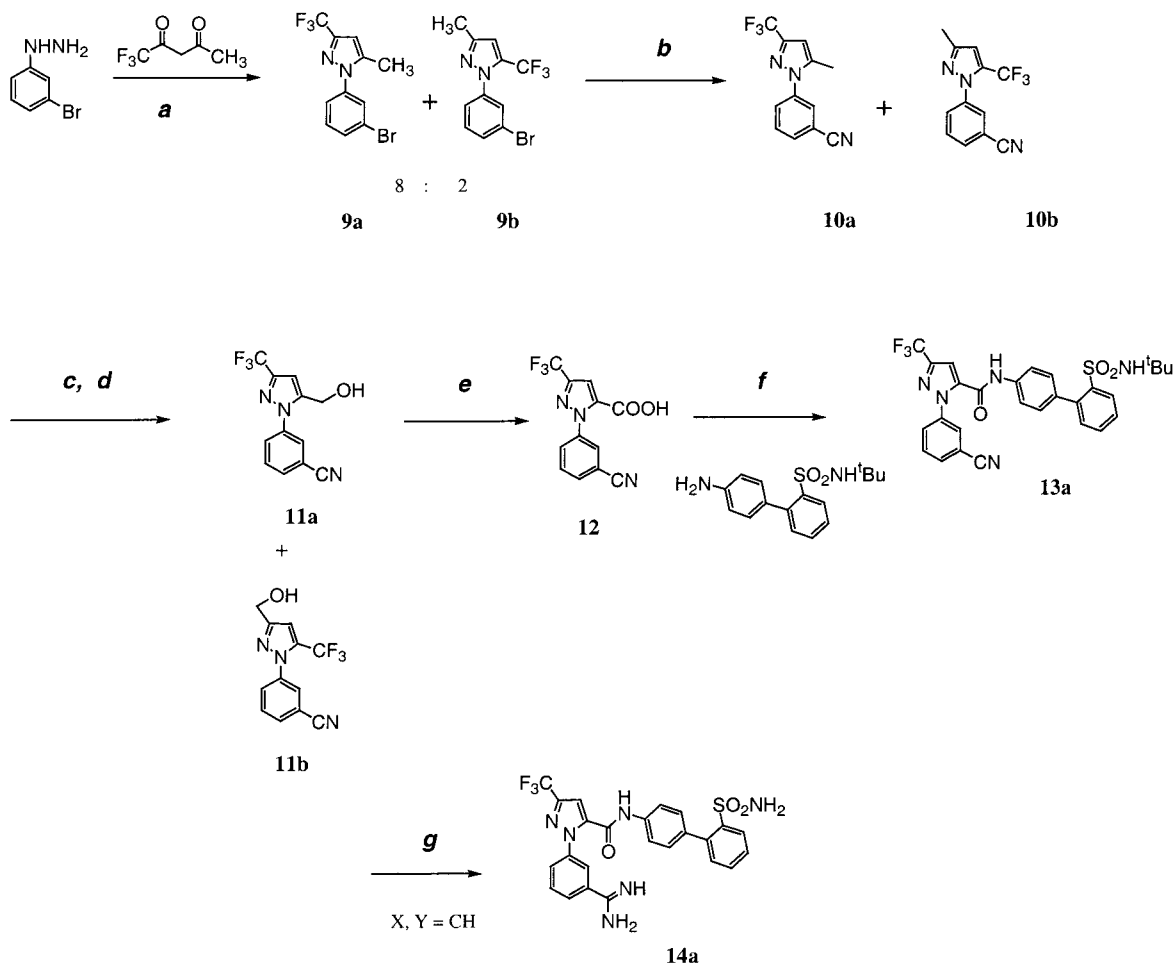
[a] (**a**) AcOH/reflux/quant; (**b**) CuCN/NMP, reflux, 40%; (**c**) NBS/CCl$_4$, quant; (**d**) CaCO$_3$/dioxane/water, 44%; (**e**) NaIO$_4$/RuCl$_3$/CH$_3$CN/H$_2$O, 90%; (**f**) oxalyl chloride/CH$_2$Cl$_2$, quant; DMAP/CH$_2$Cl$_2$, 58%; (**g**) MeOH/HCl, ammonium carbonate/MeOH, TFA, 80 °C, 46%.

The synthesis of the pyrrole analogues **3a** and **3b** is shown in Scheme 4. Condensation of 3-aminobenzonitrile with 2,5-dimethoxytetrahydrofuran afforded the pyrrole intermediate **15a**.[24] Pyrrole **15a** was formylated (POCl$_3$/DMF) regioselectively at the 2-position to derivative **15b** which was then oxidized (potassium permanganate/acetone/water) to afford the desired carboxylic acid **15c** in good yield. To prepare the 3-bromopyrrole intermediate **15d**, the 2-formyl intermediate **15b** was first brominated regioselectively at the 3-position with NBS and then oxidized to the carboxylic acid as described above. Acid chloride coupling of either **15c** or **15d** with 4′-amino[1,1′-biphenyl]-2-*tert*-butylsulfonamide afforded intermediates **16a** and **16b** which after the Pinner reactions provided pyrrole analogues **3a,b**.
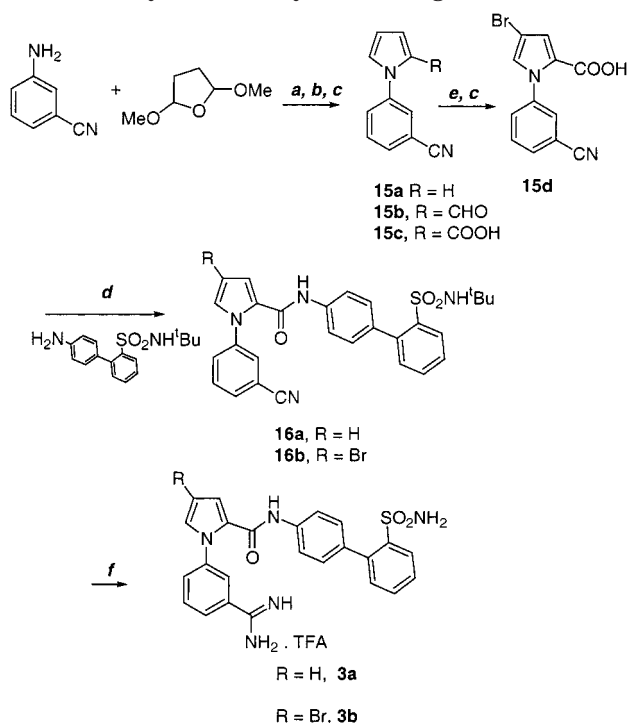
The benzonitrile precursors obtained as per Scheme 2 or 3 were subjected to reduction in a methanol-acetic acid medium using a Parr Shaker apparatus with catalytic palladium on carbon (5%) at 40 psi to afford benzylamine analogues **17a**–**h** (Scheme 5). Deprotection of the *tert*-butylsulfonamide protecting group with trifluoroacetic acid at 80 °C for 15 min afforded the requisite primary benzylamine analogue **17a**. Derivatives not containing a sulfonamide functionality were purified directly after reduction with palladium. Compound **17h** was dissolved in absolute methanol, and dry HCl gas was bubbled through the mixture for 15 min. DPC423 was obtained from this mixture by precipitation

with diethyl ether followed by recrystallization with methanol and ethyl acetate. Alternatively, **17h** was neutralized with aqueous sodium hydroxide (1 N) and subjected to the methodology described above to obtain DPC423.

Results and Discussion

Based on modeling experiments,[19] a pyrazole template was chosen to mimic the isoxazole core in compound **1**. Figure 2 shows an overlap of pyrazole **2a** with isoxazole **1** in the fXa active site. Pyrazole **2a** with a fXa K_i of 0.16 nM is equipotent to isoxazole **1** (fXa K_i = 0.15nM). On the basis of these data, it appears that the isoxazole oxygen atom does not offer any binding advantages. Additionally, pyrazole **2a** offers the potential of substitution at the 3-position, which is not possible with the isoxazole core.

The 3-methylpyrazole analogue **2b** is an order of magnitude more potent than pyrazole **2a** (fXa K_i = 13 pM compared to 0.16 nM). Furthermore, the potency of **2b** compares favorably to the very potent and naturally occurring tick anticoagulant protein (TAP, fXa K_i = 100 pM).[20] Compound **2b** shows >1000-fold selectivity for fXa compared to thrombin and trypsin (Table 1). The X-ray structure of pyrazole **2b** complexed to bovine trypsin was determined (Figure 3).[21−23] The structure has been refined to a crystallographic R-factor of 19.2% at 1.80 Å resolution. As expected, the benzamidine P$_1$

Scheme 4. Synthesis of Pyrrole Analogues **3a** and **3b**[a]

Figure 2. Overlay of pyrazole **2a** and SA862 in factor Xa.

[a] (**a**) AcOH reflux, 93%; (**b**) DMF/POCl$_3$, 0 °C−reflux, 83%; (**c**) KMnO$_4$, acetone/water, 74%; (**d**) oxalyl chloride, quant, DMAP/CH$_2$Cl$_2$, 80%; (**e**) NBS/THF, rt, 53%; (**f**) HCl/MeOH, ammonium carbonate/MeOH, 60%; TFA, 80 °C, 70%.

forms a bidentate interaction with Asp-189 (2.9 Å and 3.0 Å in the S$_1$ specificity pocket). The dihedral angle between the pyrazole and the benzamidine P$_1$ substituent is 70°, which enables the pyrazole N-2 nitrogen to interact with the backbone NH of Gln-192 (3.2 Å) and form a Van der Waal interaction with Cys-220 (3.3 Å). The 3-methyl substituent on the pyrazole is near the solvent accessible surface at the outer ridge of the active site and within contact distance of Gly-218 and Cys-220. The amide carbonyl oxygen interacts with the NH of Gly-216 (3.2 Å) and also with Ser-214 (3.0 Å) through a bridging water molecule. Similarly, the amide NH
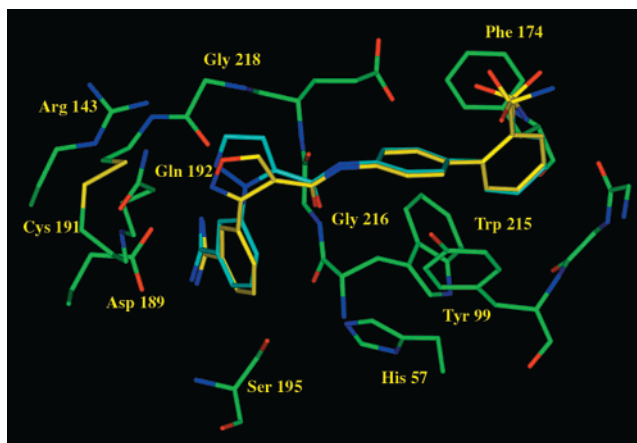
interacts with Gly-218 (3.1 Å) through a bridging water molecule. The P$_4$ *o*-biphenylsulfonamide substituent is situated in the S$_4$ region with the terminal phenylsulfonamide ring forming an edge to face interaction with Trp-215. Overall, the conformations adopted by the trypsin bound inhibitor and that predicted by the binding of pyrazole analogue **2a** in the active site of fXa are similar.

To address the importance of substitution on the core template, we examined the fXa activity of pyrrole analogues **3a** and **3b**. The 5-fold loss in fXa potency for pyrrole analogue **3a** compared to pyrazole **2a** confirms that the N-2 nitrogen in the pyrazole ring is indeed important for potency. The 3-bromo pyrrole **3b** analogue while more potent than **3a** is still significantly less potent than the 3-alkyl substituted pyrazoles **2b** and **2c**.

The N-methylation of the central amide linker as in **2d** resulted in >800-fold loss of factor Xa potency compared to the secondary amide analogue **2b**. It is possible that the loss in fXa activity is due to a change in the amide bond conformation brought about by the *N*-methyl substitution. Further work is currently being pursued to determine the importance of the amide NH and will be reported in due course.

Scheme 5. Synthesis of Benzylamine P$_1$ Analogues
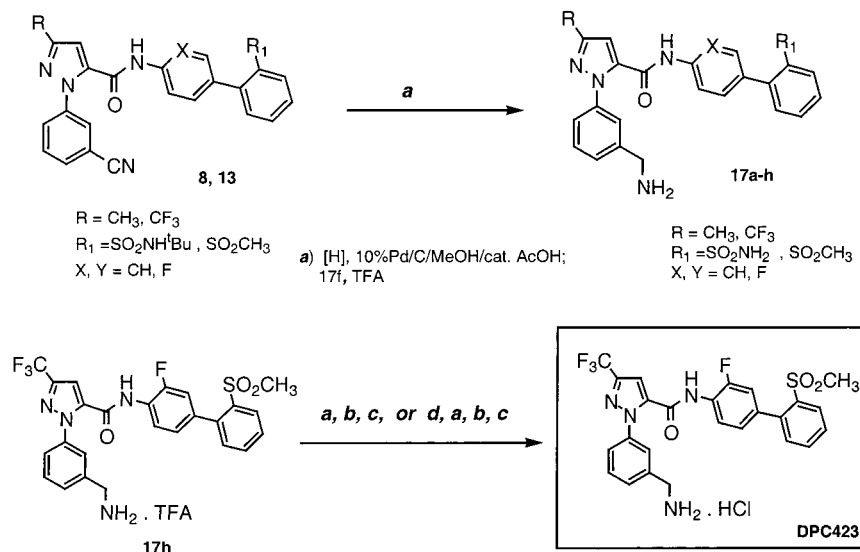
[a] (**a**) MeOH, 0 °C, HCl(gas) 0.15 min; (**b**) diethyl ether; (**c**) recrystallized, MeOH/EtOAc or (**d**) neutralize, NaOH (1 N).

**Table 1.** Comparison of SA862 with Pyrazole and Pyrrole Analogues
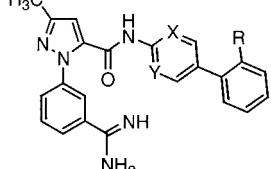

SA862   **Pyrazoles 2a-d**

Pyrroles 3a,b

compd[b]	R	human in vitro FXa[a] K_i, nM	human in vitro thrombin[a] K_i, nM	human in vitro trypsin[a] K_i, nM
isoxazole				
SA862 (**1**)		0.15	2800	21
pyrazoles				
2a	H	0.16	900	15
SN429 (**2b**)	Me	0.013	300	16
2c	n-Bu	0.06	300	11
2d N-Me amide	Me	11.00	>2000	>1600
pyrroles				
3a	H	0.80	900	56
3b	Br	0.29	300	32

[a] Human purified enzymes were used. K_i values are averaged from multiple determinations ($n = 2$), and the standard deviations are <30% of the mean. K_i's were measured as in ref 14a,b. [b] All compounds gave satisfactory analytical data (C, H, N; ±0.4% of theoretical values).
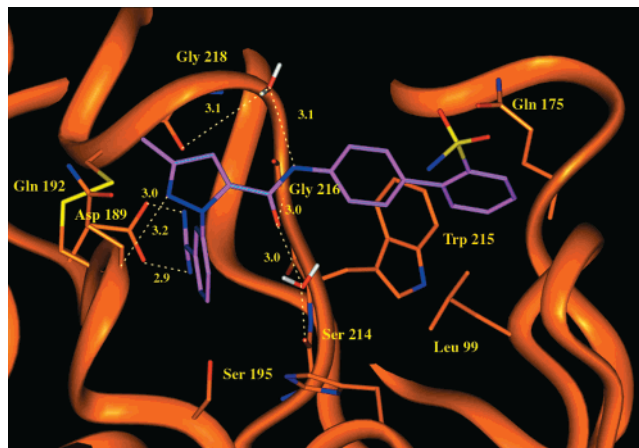
Figure 3. X-ray structure of pyrazole **2b** in bovine trypsin.

P$_4$ Modifications. In the isoxazoline series,[14] the *o*-biphenylsulfonamide moiety and the corresponding *o*-biphenylmethylsulfone were identified as optimal P$_4$ substituents. The potent fXa binding activity shown for these compounds is due to the highly constrained orientation, in which the P$_1$ benzamidine and the P$_4$ biphenylsulfonamide substituents are in a 1,3-relationship on the isoxazoline core. In these examples, the terminal phenyl ring of the 2′-biphenylsulfonamide P$_4$
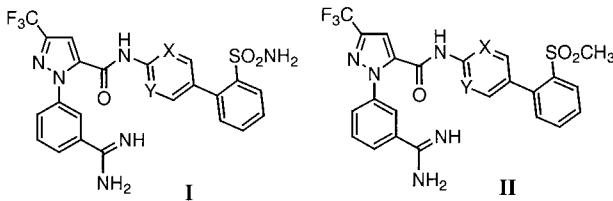
Table 2. In Vitro Activity Profile of P$_4$ Variants in the 3-Methylpyrazole Series

compd	X	Y	R	human in vitro FXa[a] K_i, nM	human in vitro thrombin[a] K_i, nM	human in vitro trypsin[a] K_i, nM
2b	CH	CH	SO$_2$NH$_2$	0.013	300	16
2e	CH	CH	SO$_2$CH$_3$	0.008	180	13
2f	CH	CH	CF$_3$	0.040	300	49
2g	CH	CH	F	0.460	450	100
2h	CH	CH	H	1.300	600	87
2i	N	CH	SO$_2$NH$_2$	0.007	1400	59
2j	N	N	SO$_2$NH$_2$	0.041	7400	150
2k	**C−F**	**CH**	**SO$_2$NH$_2$**	**0.005**	**210**	**4.6**
2l	C−Br	CH	SO$_2$NH$_2$	0.010	200	17
2m	C−Cl	CH	SO$_2$NH$_2$	0.009	300	15
2n	**C−F**	**CH**	**SO$_2$CH$_3$**	**0.020**	**230**	

[a,b] Refer to Table 1.

is orthogonal to the inner phenyl ring, forming an edge-to-face interaction with Trp-215. This orthogonal arrangement places the sulfonamide or the sulfone substituent in close proximity to the OH group of Tyr-99. In the case of the isoxazole and pyrazole series, the P$_1$ and the P$_4$ substituents are 1,2-substituted on the heterocycle. The rigid framework adopted by these inhibitors are complementary to the fXa active site and places the P$_4$ substituent in a highly optimized fashion in the S$_4$ region. Table 2 summarizes the fXa activity of additional substituted P$_4$ biaryl, pyridylphenyl, and pyrimidylphenyl pyrazole analogues. In the biaryl series, the order of potency for the 2′-substituted biphenyl P$_4$ substituents is SO$_2$CH$_3$ ≥ SO$_2$NH$_2$ > CF$_3$ > H. While the rank order of potency for these compounds is similar to that previously determined for the isoxazoline series,[14] the pyrazoles are significantly more potent. Substitution at the 3-biphenyl position (proximal phenyl) was clearly shown to affect the potency of the isoxazoline and isoxazole analogues. In the pyrazole series, the introduction of a 3-fluoro (**2k**) substituent on the proximal phenyl ring or the replacement of this ring with a 2-pyridyl ring (**2i**) results in a 2−3-fold enhancement in potency. In general, the 3-halogen biphenyl substituents improve potency in the order of F > Cl ≥ Br > H. The pyrimidyl analogue (**2j**) shows a slight loss in activity when compared to **2b** or **2i**, but it is still considerably more potent than pyrazole **2a**. The substituted biaryl analogues show good selectivity for fXa compared to thrombin but are less selective over trypsin. However, improved trypsin selectivity is observed for the aza P$_4$ analogues **2i** and **2j**. Thus, in the 3-methyl-pyrazole series, the combination of either a 3-fluoro substitution on the proximal phenyl ring or the 3-pyridyl substitution, with either an *o*-methylsulfone or *o*-sulfonamide substituent on the terminal P$_4$ phenyl ring, is considered optimal for potency or selectivity or both.

Substitution on Pyrazole Core. The replacement of the 3-methyl substituent with a longer substituent, such as butyl analogue **2c** (Table 1), results in a 2-fold loss in potency, albeit still 3-fold more potent than the

Table 3. In Vitro Activities Profile of P$_4$ Variants in the 3-Trifluoromethylpyrazole Series

| compd	I/II	X	Y	human in vitro FXa[a] K_i, nM	human in vitro thrombin[a] K_i, nM	human in vitro trypsin[a] K_i, nM
2b		CH	CH	0.013	300	16
2k		C−F	CH	0.005	210	4.6
14a	I	CH	CH	0.015	40	3.9
14b	I	N	CH	0.009	400	59
14c	I	N	N	0.010	900	20
14d	I	C−F	CH	<0.005	120	4.0
14e	II	CH	CH	0.008	70	4.3
14f	II	C−F	CH	<0.005	50	3.4

[a,b] Refer to Table 1.

Table 4. Dog Pharmacokinetics and Antithrombotic Efficacy of Benzamidine Analogues

compd	Cl (L/kg/h)[a]	V_{dss} (L/kg)[a]	$t_{1/2}$ (h)[a]	F% (po)[b]	Caco-2[c] $P_{app} \times 10^{-6}$ cm/s	rabbit A-V shunt[d] ID$_{50}$ (μmol/kg/h)
2b	0.67	0.29	0.82	4	0.30	0.02
2f	0.47	0.47	3.72	NT	NT	0.24
2i	0.76	0.21	0.31	<1	NT	0.07
2j	0.36	0.20	3.32	<5	NT	0.03
14c	0.33	0.25	1.40	NT	0.10	NT
14f	1.10	3.80	3.80	0	0.20	NT

[a] Dose of 1 mg/kg IV. [b] Oral dose of 4 mg/kg. [c] Reference 27. [d] Reference 26.

unsubstituted pyrazole **2a**. Since the methyl analogue **2b** shows much better potency than the longer chain alkyl substitutions, the 3-trifluoromethyl pyrazole was prepared. Although it was anticipated that the trifluoromethyl substituent would exhibit a better hydrophobic interaction with the fXa enzyme than the 3-methyl substituent, the 3-trifluoromethylpyrazole *o*-biphenylsulfonamide P$_4$ analogue **14a** (Table 3) and the corresponding 3-methylpyrazole analogue **2b** were found to have similar potency. Comparable potencies were also observed for the respective pyridyl analogues **14b** and **2i**. However, in the pyrimidyl series, a 4-fold improvement was observed for the trifluoromethyl pyrimidyl analogue **14c** compared to the corresponding methyl analogue **2j**. A similar enhancement was also observed for the 3-fluoro analogue **14d**. The methylsulfonyl analogue **14e** was 2-fold more potent than the corresponding sulfonamide **14a**, and as anticipated, a further increase in affinity was observed with the 3-fluoro analogue **14f**. Compounds **14d** and **14f** clearly suggest that the 3-trifluoromethyl substituent, when taken together with an optimized biaryl P$_4$ moiety, results in extremely high affinity molecules. These two compounds are currently the most potent fXa inhibitors reported in the literature to date.
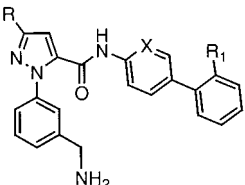
In Vivo Profile of Benzamidine Analogues. The pharmacokinetic profiles for a select set of benzamidine analogues were determined (Table 4). When dosed intravenously in beagle dogs, the biaryl P$_4$ analogues **2f** and **2i** have relatively low clearance and moderate
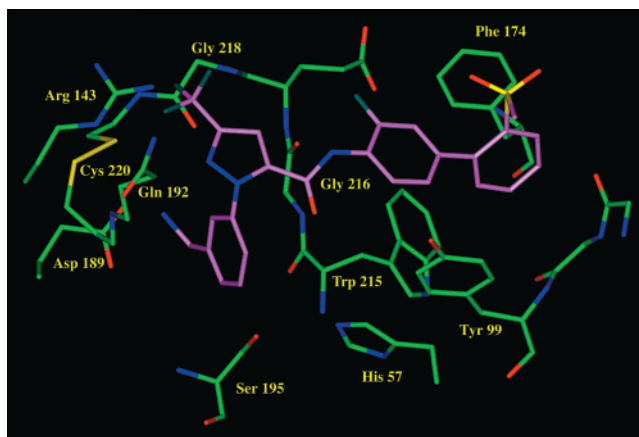
Figure 4. Binding model of pyrazole **17h** in factor Xa.

half-lives ranging from 0.3 to 3.7 h. The pyrimidyl P$_4$ analogues **2j** and **14c** show lower clearance than the other compounds evaluated but still show moderate duration of action due to their relatively low volume of distribution. The analogue **14f** has slightly higher clearance than the other compounds in this set, but it also has a higher volume of distribution and longer half-life (3.8 h). When administered orally, these benzamidine analogues show poor oral bioavailability (<5%). The poor permeability is likely a result of the highly charged amidine functionality (pK_a ~ 10.7), which was predicted based on the low Caco-2 permeability coefficient P_{app} values obtained for these compounds.
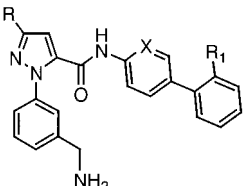
The antithrombotic efficacy of a number of benzamidine analogues was evaluated in a rabbit arteriovenous shunt thrombosis model (Table 4).[26] These compounds were administered by intravenous infusion, and the antithrombotic effect was measured as the ID$_{50}$ (dose which reduced clot weight by 50%). In this assay, pyrazole analogues **2b**, **2f**, **2i**, and **2j** inhibit thrombus formation in a dose dependent manner with ID$_{50}$'s ranging from 0.23 μmol/kg/h to 0.02 μmol/kg/h.

Benzylamine P1 Analogues. To improve the oral absorption of the pyrazole analogues, we adopted a strategy of replacing the P$_1$ benzamidine with a less basic moiety (preferably with pK_a < 10). One of the first benzamidine replacements considered was the benzylamine moiety (pK_a of ~8.8). We modeled the benzylamine analogue **17h** in the active site of fXa (Figure 4) and determined that the conformation assumed by **17h** was very similar to that seen for benzamidine **2b**. In the case of the benzylamine analogue **17h**, the single amino functionality interacts with Asp-189, but is not capable of a bidentate interaction such as that seen for the benzamidine analogue **2b**. In addition, since no interaction is observed with Ser-190, some loss in fXa activity was expected. Since the pyrazole series was optimized to the 5−10 pM range, we were able to sacrifice up to 2 orders of magnitude in potency in exchange for compounds with improved oral absorption. The in vitro data for the benzylamine analogues **17a−d** is reported in Table 5. A quick review of the data shows similar fXa potency trends as seen in the benzamidine series. The benzylamine analogue **17a** (fXa K_i = 2.5 nM) is 190-fold less potent than its benzamidine counterpart **2a** (fXa K_i = 0.013 nM). The incorporation of a 3-F substituent in the proximal phenyl ring resulted in **17b** with a modest improvement in potency (fXa K_i = 1.6

Table 5. Profile of Pyrazole Benzylamine P_1 Analogues

compd	R	X	R_1	human in vitro FXa[a] K_i, nM	human in vitro thrombin[a] K_i, nM	human in vitro trypsin[a] K_i, nM	rabbit A-V shunt[b] ID_{50} (μmol/kg/h)	human APTT, μM	HPB[c]
2b (amidine)	**CH₃**	**CH**	**SO₂NH₂**	**0.013 (0.03)**[d]	**300**	**16**	**0.02**	**0.44**	**70**
17a	CH₃	CH	SO₂NH₂	2.70 (4.10)[d]	21000	250	NT	2.30	63
17b	CH₃	C−F	SO₂NH₂	1.60 (2.20)[d]	12000	120	NT	0.92	70
17c	CH₃	CH	SO₂CH₃	0.89	21000	220	NT	1.30	NT
17d	CH₃	C−F	SO₂CH₃	0.48 (1.20)[d]	14000	130	0.90	1.10	75
17f (amidine)	**CF₃**	**C−F**	**SO₂CH₃**	**<0.005**	**50**	**3.4**	**NT**		**NT**
17e	CF₃	CH	SO₂NH₂	0.91 (2.10)[d]	14000	120	1.00	6.40	83
17f	CF₃	C−F	SO₂NH₂	0.36 (1.00)[d]	2000	53	0.60	0.91	93
17g	CF₃	CH	SO₂CH₃	0.38	5800	100	2.20	2.20	77
17h	CF₃	C−F	SO₂CH₃	0.15 (0.30)[d]	6000	60	1.10 (0.15)[e]	4.86	89

[a] Refer to Table 1. [b] Reference 26. [c] HPB refers to human protein binding; all compounds gave satisfactory analytical data including C, H, N within ± of theoretical values. [d] Rabbit in vitro data. [e] IC_{50}, which is the concentration to inhibit thrombus formation by 50% in rabbits.

Table 6. Dog Pharmacokinetic Profile of Benzylamine Analogues

compd	X	R_1	Cl (L/kg/h)	V_{dss} (L/kg)	$t_{1/2}$ (h)	F% (po)	Caco-2[a] $P_{app} \times 10^{-6}$ (cm/s)
			R = CH₃				
2b (amidine)	**CH**	**SO₂NH₂**	**0.67**	**0.29**	**0.82**	**4.40**	**0.30 ± 0.07**
17a	CH	SO₂NH₂	0.43	1.90	9.30	13	0.20 ± 0.03
17b	C−F	SO₂NH₂	0.30	0.60	2.80	10	0.95 ± 0.02
17c	CH	SO₂CH₃	0.98	3.62	5.80		1.20 ± 0.09
17d	C−F	SO₂CH₃	2.10	3.10	1.90	73	3.14 ± 0.10
			R = CF₃				
14f (amidine)	**C−F**	**SO₂CH₃**	**1.10**	**3.80**	**3.80**	**<1**	**0.20 ± 0.01**
17e	CH	SO₂NH₂	0.75	4.36	7.88	35	bql
17f	C−F	SO₂NH₂	0.10	0.34	4.70	22	0.91 ± 0.11
17g	CH	SO₂CH₃	0.44	5.82	9.50	39	3.38 ± 0.08
17h	C−F	SO₂CH₃	0.24	0.90	7.50	57	4.86 ± 0.33

[a] IV dose = 0.5 mg/kg. [b] Oral dose = 0.2 mg/kg. [c] Reference 27.

nM) and improved permeability in the Caco-2 assay with a P_{app} value of 0.95×10^{-6} cm/s compared to 0.2×10^{-6} cm/s (Table 6). Replacing the 2′-sulfonamide on the terminal phenyl ring with the 2′-sulfonylmethyl substituent afforded **17c** (fXa K_i = 0.89 nM). This series was further optimized by incorporating the 3-fluoro substituent (**17d**; fXa K_i = 0.48 nM). Most notable was the improvement in the Caco-2 permeability displayed by analogues **17c** and **17d**, which have P_{app} values of 1.20×10^{-6} cm/s and 3.14×10^{-6} cm/s, respectively (Table 6). The introduction of the trifluoromethyl pyrazole into the benzylamine P_1 series provides compounds with improved potency and an SAR which parallels that observed for the methylpyrazole benzylamine P_1 series. The most potent compound was **17h** (K_i = 0.15 nM) which contains the same P_4 substituent as **17d**. More importantly the Caco-2 permeability for

17h ($P_{app} = 4.86 \times 10^{-6}$ cm/sec) improves significantly. All compounds produced good selectivity ratios for fXa relative to thrombin and trypsin. Against relevant human enzymes, **17h** showed greater than 10000-fold selectivity for inhibition of fXa over thrombin and 300-fold selectivity over trypsin and kallikrein.[29] In the activated partial thromboplastin time (APTT) in vitro clotting assay, the methylpyrazole benzylamine P_1 analogues (Table 5) displayed clotting times within 2- to 3-fold when compared to benzamidine **2b** and are slightly higher for the trifluoromethyl analogues. The higher protein binding exhibited by the trifluoromethyl pyrazole analogues (Table 5) over their 3-methyl pyrazole counterparts may account at least in part for these changes. In the rabbit arterio-venous shunt thrombosis model, the benzylamine analogues exhibit good antithrombotic potency with ID_{50} values in the range of 0.6−
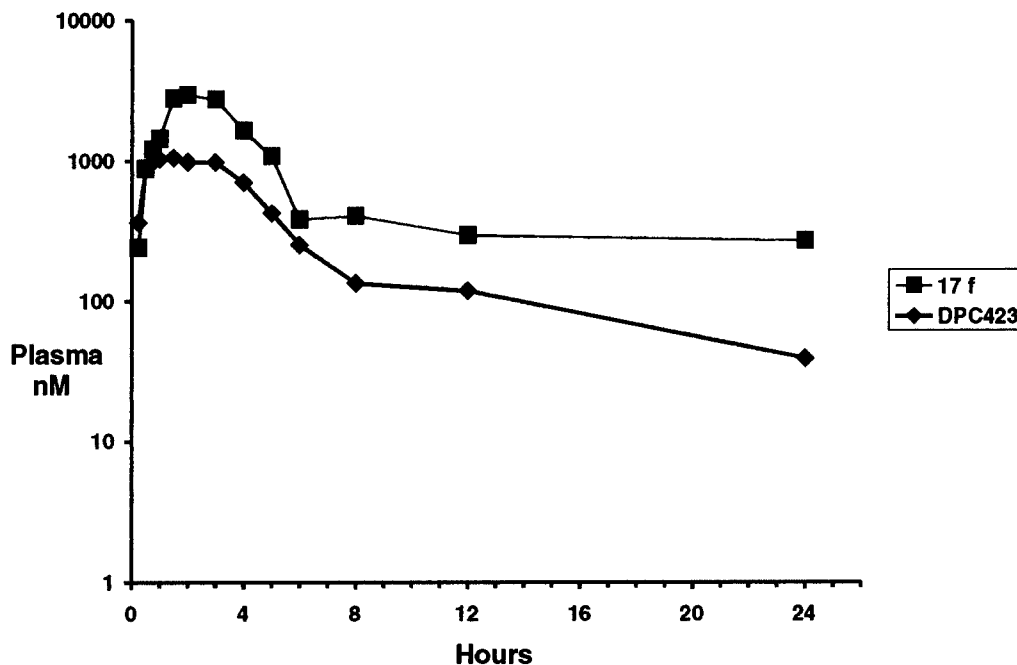
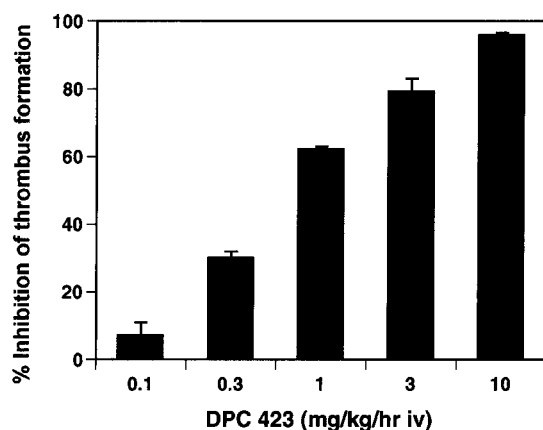**Figure 5.** In vivo dog pharmacokinetics of DPC423 (**17h**) and **17f**.

Figure 6. Antithrombotic effect of DPC423 (**17h**) in the rabbit arterio-venous shunt thrombosis model.

2.2 μmol/kg/h (Table 5). With the high binding affinity and good selectivity relative to thrombin and trypsin coupled with the good Caco-2 permeability and anti-thrombotic potency for these benzylamine analogues in hand, we next addressed the pharmacokinetic properties of the benzylamines.

Pharmacokinetic Profile of Benzylamine Analogues. When methyl pyrazole sulfonamide **17a** was dosed via intravenous administration to beagle dogs, low clearance and long half-life were observed (Table 6). However, when dosed orally the compound demonstrated relatively low oral availability, again consistent with the low measured Caco-2 permeability. The 3-fluoro analogue **17b** also displayed low clearance and poor oral absorption profile. Good oral bioavailability (73%) was seen for **17d**. Unfortunately, the high clearance and short duration of action made this compound unsuitable for further evaluation. Most of the 3-tri-fluoromethylpyrazole benzylamine analogues show good oral absorption and significantly longer duration of action. The best profile was observed with **17h**, which had a lower clearance (0.24 L/kg/h) and a slightly larger volume of distribution (V_{dss}) than the corresponding

Table 7. Selectivity Profile for DPC423 (**17h**)
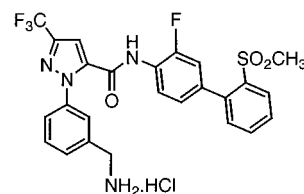
DPC 423

human enzymes	K_i (nM)
factor Xa	0.15 ± 0.02
trypsin	60 ± 6.5
thrombin	6000
plasma kallikrein	61[a]
activated protein C	1800[a]
factor IXa	2200 ± 0.2[a]
factor VIIa	>15000[a]
chymotrypsin	>17000[a]
urokinase	>19000[a]
plasmin	>35000[a]
tPA	>45000[a]
complement factor I IC$_{50}$	44000[a]

[a] Data from **17h** TFA salt, others from HCl salt.

sulfonamide **17f**. These differences resulted in a longer exposure ($t_{1/2}$ of 7.5 h compared to 4.7 h) (Figure 5). When dosed orally, **17h** showed higher oral bioavailability (F% = 57%) compared to the corresponding sulfonamide **17f** (F% = 22%) and the des-fluoro analogue **17g** (F% = 39%; Table 6).

In rats, a higher total body clearance (5.1 ± 0.75 L/h/kg) and V_{dss} (21 ± 1.9 L/kg) was observed for 17 h. The terminal elimination half-life in rats was 4.6 ± 0.7 h (mean $\pm$ SD; $n = 3$). When dosed orally to rats, the plasma concentrations are lower and more variable than those encountered in dogs. The apparent oral bioavailability of **17h** in rats is 36%.

Compound **17h** was shown to be 89% protein bound as measured in human plasma by equilibrium dialysis. In the rabbit arterio-venous shunt thrombosis model, the compound inhibits thrombus formation with an ID$_{50}$

= 1.1 μmol/kg/h and with a IC$_{50}$ (concentration to inhibit thrombus formation by 50%) value of 0.15 μM (Figure 6).[30] The IC$_{50}$ value obtained for **17h** in the rabbit thrombosis models reflects its potency in this model.[31] Overall, compound **17h** showed the best balance of good permeability resulting in good oral bioavailability, low clearance, and relatively long half-life. When combined with its exceptionally good fXa potency and selectivity, **17h** emerged as an ideal candidate for further development as an antithrombotic agent (Table 7). DPC423, a crystalline nonhygroscopic hydrochloride salt form of **17h**, was selected for clinical development.

Conclusions

Optimization of the core template of our fXa inhibitors led to a highly potent pyrazole analogue **2b**. Further optimization resulted in benzamidine analogues such as **14d** and **14f**, which are the most potent fXa inhibitors reported in the literature to date. While the benzamidine analogues demonstrated good factor Xa potency and selectivity, poor oral bioavailability and relatively short duration of action precluded further development of these compounds. Incorporation of a less basic benzylamine P$_1$ with a pK_a of ~8.8, followed by careful SAR manipulations resulted in the identification of analogue **17h**, a highly potent, selective, and orally bioavailable inhibitor of fXa. This compound is a potent antithrombotic agent which inhibits thrombus formation in a dose dependent manner. The nonhygroscopic hydrochloride salt form DPC423 was selected for clinical development.

Experimental Section

Preparations of the final products and intermediates are included as Supporting Information. All reactions were run under an atmosphere of dry nitrogen. All solvents were used without purification as acquired from commercial sources. NMR spectra were obtained with a Varian VXR-300a spectrometer. Microanalyses were performed by Quantitative Technologies Inc. and were within 0.4% of the calculated values. Mass spectra were obtained on a HP 5988A MS/HP particle beam interface. Flash chromatography was done using EM Science silica gel 60. HPLC purifications were performed on a Ranin Dynamax SD200 instrument using a C18 reverse phase column with acetonitrile/water (containing 0.05% TFA) as a mobile phase. HPLC purity in most cases was >95%. Various P4 starting materials such as 4′-amino[1,1′-biphenyl]-2-*tert*-butylsulfonamide, 4′-amino-3′-fluoro[1,1′-biphenyl]-2-*tert*-butylsulfonamide, 3-fluoro-2′-(methylsulfonyl)[1,1′-biphenyl]-4-amine, 2-(6-amino-3-pyridinyl)benzene-*tert*-butylsulfonamide, 2-(6-amino-3-pyrimidinyl)benzene-*tert*-butylsulfonamide substituted aminobiaryls, and aminopyridylphenylsulfonamides were obtained as per procedures described by Quan.[14a–c]

Ethyl-1-(3-cyanophenyl)-3-methyl-1*H*-pyrazole-5-carboxylate (4a) and 1-(3-Cyanophenyl)-3-methyl-1*H*-pyrazole-5-carboxylic Acid (4b). A solution of 3-cyanophenylhydrazine hydrochloride (3.38 g, 19.98 mmol) and methyl-4-(dimethylamino)-2-oxo-3-butenoate (3.14 g, 19.98 mmol) in acetic acid (75 mL) was refluxed for 18 h. The solution was concentrated and the residue chromatographed on silica gel (hexane/ethyl acetate, 8:2) to afford the desired pyrazole regioisomer **4a** (0.81 g, 17%). LRMS (ESI$^+$): 242 (M + H). ^{1}H NMR (CDCl$_3$) δ: 3.77 (s, 3H), 4.20 (q, 2H), 7.16 (d, J = 1.5 Hz, 1H), 7.68 (t, 1H), 7.84 (m, 2H), 7.92 (dd, J = 2 and 8 Hz, 1H), 8.08 (d, J = 2.1 Hz, 1H). The above solid was saponified with LiOH (0.010 g, 0.2 mmol) in a THF/water solution (4:1, 25 mL). The reaction mixture was acidified with HCl (1 N), and the organics were extracted with ethyl acetate (2 × 50 mL), dried (magnesium sulfate), and evaporated to a colorless solid **4b** (0.70 g, 98%). LRMS (ESI$^+$): 214 (M + H). ^{1}H NMR

(CDCl$_3$) δ: 7.16 (d, J = 1.5 Hz, 1H), 7.68 (t, 1H), 7.84 (m, 2H), 7.92 (dd, J = 2 and 8 Hz, 1H), 8.08 (d, J = 2.1 Hz, 1H).

1-{3-[Amino(imino)methyl]phenyl}-*N*-[2′-(aminosulfonyl) [1,1′-biphenyl]-4-yl]-3-methyl-1*H*-pyrazole-5-carboxamide, Trifluoroacetic Acid Salt (2a). The pyrazole **4b** (0.20 g, 0.92 mmol) was coupled according to the method described by Quan et al.[14b,c] to 4′-amino[1,1′-biphenyl]-2-*tert*-butylsulfonamide (0.28 g, 0.92 mmol) to afford **5** (0.36 g, 76%). LRMS (ESI$^+$): 500 (M + H)$^+$. ^{1}H NMR (CDCl$_3$) δ: 1.04 (s, 9H), 3.88 (s, 1H), 7.05 (s, 1H), 7.18–7.37 (m, 3H), 7.59–7.77 (m, 4H), 7.83 (dd, J = 2.5 and 8 Hz, 1H), 7.80 (m, 2H), 8.02 (m, 2H). Compound **5** was dissolved in dry methanol (10 mL) and cooled to 0 °C. Into this solution was bubbled dry HCl gas for 15 min. The reaction mixture was sealed and stirred at room temperature for 18 h. Removal of solvents in vacuo afforded the imidate intermediate which was immediately treated with a saturated solution of ammonia in methanol (10 mL). The reaction mixture was stirred at room temperature for 12 h, concentrated, and the crude benzamidine purified by reverse phase HPLC to afford 0.15 g of pyrazole benzamidine **2a** (45%) as the TFA salt. LRMS (ESI$^+$): 461 (M + H). ^{1}H NMR (DMSO-d_6) δ: 7.23–7.38 (m, 5H), 7.56–7.78 (m, 5H), 7.80–7.86 (dt, J = 1.4 and 10 Hz, 2H), 7.93 (d, J = 1.9 Hz, 1H), 8.01 (dd, J = 1.9 and 12 Hz, 2H), 9.06 (bs, 2H), 9.45 (bs, 2H), 10.70 (s, 1H). HRMS (C$_{23}$H$_{20}$N$_6$O$_3$S): calcd 461.2678; found, 461.2587. HPLC purity >95%. Anal. calcd for C$_{23}$H$_{20}$N$_6$O$_3$S·1.3TFA·0.2H$_2$O: C, 50.21, H, 3.57, N, 13.72; found, C, 50.11, H, 3.65, N, 13.88.

Ethyl-1-(3-cyanophenyl)-3-methyl-pyrazol-5-yl-carboxylate (6). Prepared in 75% yield following the methodology of Ashton.[18] LRMS (CI/NH$_3$): 256 (M + H). 1H NMR (CDCl$_3$) δ: 1.31 (t, 3H), 2.36 (s, 3H), 4.3 (q, 2H), 6.86 (s, 1H), 7.58 (t, 1H), 7.70 (dd, 1H), 7.76 (t, 1H).

1-(3-Cyanophenyl)-3-methyl-1*H*-pyrazol-5-ylcarboxylic Acid (6a). Ethyl-1-(3-cyanophenyl)-3-methyl-pyrazol-5-yl-carboxylate (0.55 g, 2.1 mmol) was dissolved in THF (20 mL) and to this was added LiOH (0.5 M, 5,6 mL). The reaction mixture was stirred at room temperature for 18 h, quenched with water (50 mL), and extracted with ethyl acetate (2 × 50 mL). The aqueous layer was acidified, and the organics were extracted with ethyl acetate (2 × 50 mL), dried (magnesium sulfate), and evaporated to afford pure acid (0.44 g, 90%). LRMS (CI/NH$_3$): 228 (M + H). ^{1}H NMR (DMSO-d_6) δ: 2.27 (s, 3H), 6.89 (s, 1H), 7.09 (t, 1H), 7.82 (dd, 1H), 7.91 (d, 1H), 8.02 (t, 1H).

1-(3-Cyanophenyl)-*N*-[2′-(*tert*-butylaminosulfonyl) [1,1′-biphenyl]-4-yl]-3-methyl-1*H*-pyrazole-5-carboxamide, Trifluoroacetic Acid Salt (8). To a dichloromethane solution (20 mL) of 1-(3-cyanophenyl)-3-methyl-pyrazol-5-yl carboxylic acid (0.2 g, 0.88 mmol) was added oxalyl chloride (0.12 mL, 1.32 mmol). The reaction mixture was stirred at room temperature for 2 h. To this solution was then added 4′-amino-[1,1′-biphenyl]-2-*tert*-butylsulfonamide (0.27 g, 0.88 mmol) and triethylamine (0.50 mL), and the reaction mixture was stirred at room temperature for 24 h. The reaction was quenched with water (50 mL), extracted with ethyl acetate (2 × 50 mL), washed with brine (50 mL), and dried (magnesium sulfate). Evaporation in vacuo afforded an oil which was chromatographed on silica gel (CH$_2$Cl$_2$:MeOH, 9:1) to afford the title compound (0.39 g, 99%). LRMS (ESI$^-$): 458 (M − H). ^{1}H NMR (CDCl$_3$) δ: 1.03 (s, 9H), 2.42 (s, 3H), 3.64 (s, 1H), 6.76 (s, 1H), 7.30 (d, 1H), 7.50 (m, 3H), 7.58 (m, 2H), 7.68 (d, J = 7.8 Hz, 3H), 7.76 (d, J = 8.2 Hz, 1H), 7.80 (d, J = 7.9 Hz, 1H), 8.05 (s, 1H), 8.16 (d, J = 8.0 Hz, 1H).

1-{3-[Amino(imino)methyl]phenyl}-*N*-[2′-(aminosulfonyl)[1,1′-biphenyl]-4-yl]-3-methyl-1*H*-pyrazole-5-carboxamide (2b). Compound **8** (0.39 g, 0.85 mmol) was dissolved in anhydrous MeOH (20 mL) saturated with HCl. The reaction mixture was stirred at room temperature for 24 h and concentrated and the residue redissolved in MeOH (20 mL). Ammonium carbonate was added (1.0 g, 10.00 mmol), and the reaction mixture was stirred at room temperature for 18 h. Concentration followed by purification of the residue via reverse phase HPLC afforded pyrazole **2b** (0.15 g, 36%). LRMS (ESI$^+$): 475 (M + H). ^{1}H NMR (DMSO-d_6) δ: 2.50 (s, 3H), 7.03

(s, 1H), 7.27 (s, 2H), 7.32 (d, $J = 8.5$ Hz, 1H), 7.37 (d, $J = 8.3$ Hz, 2H), 7.62 (m, 2H), 7.70 (d, $J = 7.8$ Hz, 2H), 7.75 (d, $J = 8.2$ Hz, 1H), 7.83 (t, 1H), 7.97 (s, 1H), 8.03 (d, 1H), 9.09 (s, 2H), 9.44 (s, 2H), 10.66 (s, 1H). HRMS ($C_{24}H_{23}N_6O_3S$): calcd 475.1552; found, 475.1537. HPLC purity >95%. Anal. calcd for $C_{24}H_{22}N_6O_3S \cdot 1.0$TFA: C, 53.06, H, 3.94, N, 14.28; found, C, 53.07, H, 3.89, N, 14.10.

1-(3-Cyanophenyl)pyrrole (15a). 2,5-Dimethoxytetrahydrofuran (0.44mol, 59.5 mL) was added to an acetic acid (200 mL) solution of 3-aminobenzonitrile (47.45 g, 0.40 mol). The solution was stirred at reflux overnight, allowed to cool to room temperature, and diluted with ethyl acetate (250 mL). The combined ethyl acetate layers were washed with brine (3 × 200 mL) and saturated sodium carbonate (200 mL), dried over magnesium sulfate, and filtered through a plug of silica gel. Evaporation in vacuo afforded the title compound (62.82 g, 93%). LRMS (H_2O–CI): 169 (M + H). ^{1}H NMR (CDCl$_3$) δ: 6.41 (t, $J = 2.2$ Hz, 2H), 7.09 (t, $J = 2.2$ Hz, 2H), 7.51–7.55 (m, 2H), 7.60–7.66 (m, 2H).

1-(3-Cyanophenyl)pyrrole-2-carboxaldehyde (15b). Phosphorus oxy-chloride (191.8 mmol, 17.90 mL) was added over 0.5 h to *N,N*-dimethylformamide (191.8 mmol, 14.1 mL) at 0 °C. The reaction mixture was cooled to 0 °C and diluted with 1,2-dichloroethane (100 mL). A solution of 1-(3-cyanophenyl)pyrrole (29.33 g, 174.4 mmol) in 1,2-dichloroethane (250 mL) was added slowly via an addition funnel, and the mixture was heated to reflux for 0.5 h. The solution was cooled to room temperature, and to this mixture were added sodium acetate (86.55 g, 1.05 mol) and water (250 mL). The solution was heated to reflux for 0.5 h, diluted with ethyl acetate (250 mL), washed with brine (25 mL) and saturated aqueous sodium carbonate (250 mL), dried over magnesium sulfate, filtered through a plug of silica gel, and evaporated in vacuo to afford a brown solid. Recrystallization with ethyl acetate afforded the title compound as tan solid (28.4 g, 83%). LRMS (NH$_3$–CI): 214 (M + NH$_4$). ^{1}H NMR (CDCl$_3$) δ: 6.44–6.47 (m, 1H), 7.07 (d, $J = 1.1$ Hz, 1H), 7.17 (dd, $J = 3.7$ and 1.5 Hz, 1H), 7.54–7.71 (m, 4H), 9.58 9s, 1H).

1-(3-Cyanophenyl)-*N*-[2′-(*tert*-butylaminosulfonyl)[1,1′-biphenyl]-4-yl]-*N*-methyl-1*H*-pyrrole-2-carboxamide, (R = H, 16a). A solution of 1-(3-cyanophenyl)pyrrole-2-carboxaldehyde (5.14 g, 26.20 mmol) and acetone/water (1:1, 300 mL) was cooled to 0 °C. To this solution was added potassium permanganate (12.42 g, 78.60 mmol) over 0.5 h, and the reaction mixture was allowed to warm to room temperature. The mixture was quenched with sodium bisulfite (10.90 g, 104.8 mmol), and the solution was made acidic with HCl (10%). The solution was filtered through a plug of Celite, extracted with ethyl acetate (3 × 100 mL), washed with brine (200 mL), dried over magnesium sulfate, and evaporated in vacuo to afford the corresponding carboxylic acid derivative **15c** (4.11 g, 74%) as a colorless solid. LRMS (ESI⁻): 211.2 (M – H). The 1-(3-cyanophenyl)pyrrole-2-carboxylic acid (2.77 g, 13.05 mmol) obtained above was dissolved in anhydrous DMF (50 mL), and to this mixture were added triethylamine (1.98 mL, 19.58 mmol), benzotriazol-1-yloxytris(dimethylamino)phosphonium hexafluoro-phosphate (8.66 g, 19.58 mmol), and 4′-amino[1,1′-biphenyl]-2-*tert*-butylsulfonamide (6.03 g, 19.84 mmol). The reaction mixture was heated at 50 °C for 18 h, cooled to room temperature, and quenched with water (200 mL). The organics were extracted with ethyl acetate (2 × 100 mL), washed with brine (100 mL), dried over magnesium sulfate, and concentrated in vacuo. Purification of the residue via flash chromatography (hexane/ethyl acetate, 3:2) afforded the title compound (1.9 g, 29%). LRMS (NH$_3$–CI): 516 (M + NH$_4$). ^{1}H NMR (CDCl$_3$) δ: 1.01 (s, 9H), 3.65 (bs, 1H), 6.38 (dd, $J = 3.7$ and 2.9 Hz, 1H), 6.96–6.98 (m, 2H), 7.28 (dd, $J = 7.7$ and 1.5 Hz, 1H), 7.43–7.49 (m, 2H), 7.51–7.66 (m, 8H), 7.94 (bs, 1H), 8.15 (dd, $J = 7.8$, 1.3 Hz, 2H).

1-{3-[Amino(imino)methyl]phenyl}-*N*-[2′-(aminosulfonyl)[1,1′-biphenyl]-4-yl]-*N*-methyl-1*H*-pyrrole-2-carboxamide, Trifluoroacetic Acid Salt (3a). To a cold (0 °C) anhydrous methyl acetate (60 mL) solution of **16a** (R = H, 0.37 g, 0.74 mmol) was added methanol (0.30 mL, 7.4 mmol).

Gaseous anhydrous HCl was bubbled through the solution for 0.5 h and allowed to stir overnight at room temperature. The reaction was concentrated in vacuo, and the residue was redissolved in anhydrous methanol (100 mL). Ammonium carbonate (0.43 g, 4.45 mmol) was added and the reaction mixture stirred overnight at room temperature. Evaporation in vacuo afforded a solid mass which was purified by reverse phase HPLC to afford the title compound as a colorless solid. LRMS: (ESI⁺): 460.3 (M + H). ^{1}H NMR (DMSO-d_6) δ: 6.39 (t, 1H), 7.15–7.17 (m, 1H), 7.20 (s, 2H), 7.25–7.31 (m, 4H), 7.48–7.57 (m, 2H), 7.60–7.64 (m, 4H), 7.74–7.78 (m, 1H), 7.84 (bs, 1H), 7.98 (dd, $J = 7.7$, 1.4 Hz), 9.14 (bs, 2H), 9.38 (bs, 2H). HPLC purity >95%. HRMS ($C_{24}H_{22}N_5O_3S$): calcd 460.1443; found, 460.1447.

1-(3-Cyanophenyl)-2-formyl-4-bromopyrrole. 1-(3-Cyanophenyl)pyrrole-2-carboxaldehyde (6.06 g, 30.89 mmol) was combined with *N*-bromosuccinimide (6.60 g, 37.06 mmol) in anhydrous CCl$_4$ (150 mL) and stirred at room temperature overnight. The residue was treated with ethyl acetate (50 mL), filtered through a silica gel, and concentrated in vacuo. The residue was then recrystallized from ethyl acetate to afford the title compound as a light brown solid (4.49 g, 53%). LRMS (CI/NH$_3$): 292 (M + NH$_4$). ^{1}H NMR (CDCl$_3$) δ: 7.06 (dd, $J = 1.8$, 0.9 Hz, 1H), 7.14 (d, $J = 2.0$ Hz, 1H), 7.57–7.60 (m, 2H), 7.62–7.63 (m, 1H), 7.72–7.75 (m, 1H), 9.52 (d, $J = 0.8$ Hz, 1H). HPLC purity >95%.

1-{3-[Amino(imino)methyl]phenyl}-*N*-[2′-(aminosulfonyl)[1,1′-biphenyl]-4-yl]-4-bromo-*N*-methyl-1*H*-pyrrole-2-carboxamide, Trifluoroacetic Acid Salt (3b). Following the procedures described above, 1-(3-cyanophenyl)-2-formyl-4-bromopyrrole was converted into the title compound. LRMS (ESI⁺): 538.2 (M + H). ^{1}H NMR (DMSO-d_6) δ: 7.21 (s, 2H), 7.24–7.30 (m, 4H), 7.51 (s, 2H), 7.54–7.57 (m, 1H), 7.62–7.66 (m, 4H), 7.77–7.80 (m, 1H), 7.86 (bs, 1H), 7.98 (d, $J = 7.3$ Hz, 1H), 9.01 (bs, 2H), 9.36 (bs, 2H); HPLC purity >95%. HRMS ($C_{24}H_{21}BrN_5O_3S$): calcd 538.054; found, 538.055.

Preparation of 1-(3-Cyanophenyl)-3-trifluoromethylpyrazole-5-carboxylic Acid (12). A solution of 1,1,1-trifluoro-2,4-pentanedione (1.35 mL, 11.2 mmol), 3-bromophenylhydrazine hydrochloride (3 g, 13.4 mmol) in glacial acetic acid (20 mL), and 2-methoxyethanol (10 mL) was heated to reflux for 2 h. The solvents were removed in vacuo, and the residue was dissolved in ethyl acetate (100 mL). The ethyl acetate solution was washed with 1 N HCl (10 mL), saturated NaHCO$_3$ (50 mL), and brine (50 mL) and dried (magnesium sulfate). Purification via silica gel flash chromatography [hexanes/ethyl acetate (8:1)] afforded the pyrazole intermediates **9a** and **9b** as a 8:2 mixture of the two isomers (3.42 g, 100%), the desired 5-methylpyrazole isomer pre-dominating. The mixture was combined with 1-methyl pyrrolidinone (7 mL) and copper cyanide (1.3 g, 14.5 mmol) and heated to reflux for 18 h. The reaction mixture was cooled to room temperature, diluted with ethyl acetate (100 mL), and filtered. The filtrate was washed with water (100 mL) and brine (50 mL) and dried (magnesium sulfate). The crude mixture was purification via silica gel flash chromatography (hexane ethyl acetate, 9:1) to afford a mixture of cyanophenyl intermediates **10a** and **10b** (1.15 g, 40%). To the mixture of **10a** and **10b** (0.65 g, 2.59 mmol) in carbon tetrachloride (20 mL) was added *N*-bromosuccinimide (0.48 g, 2.7 mmol) and benzoylperoxide (20 mg). The reaction mixture was refluxed for 6 h, cooled, filtered, and concentrated to yield the crude bromide. The bromide was dissolved in a mixture of dioxane/water (1:1, 20 mL), and calcium cabonate (0.46 g, 4.6 mmol) was added. The solution was heated on a steam bath for 6 h, cooled, filtered, and concentrated in vacuo. Purification via silica gel flash chromatography (hexanes/ethyl acetate, 1:1) afforded the desired alchohol **11a** (0.31 g, 44%). LRMS (CI–NH$_3$): 268.1 (M + H), 285 (M + NH$_4$). ^{1}H NMR (CDCl$_3$) δ: 8.07 (s,1H), 8.01 (dd, $J = 2.2, 8.05$ Hz, 1H), 7.77 (d, $J = 7.7$ Hz, 1H), 7.68 (t, $J = 8.05$ Hz, 1H), 6.76 (s,1H), 4.72 (d, $J = 5.85$ Hz, 2H), 2.02 (t, $J = 5.86$ Hz, 1H). To **11a** (0.18 g, 0.67 mmol) in acetonitrile (5 mL) was added sodium periodate (0.3 g, 1.4 mmol), water (5 mL), and a crystal of ruthenium(III)chloride hydrate. The reaction

was stirred for 18 h at room temperature, filtered, and concentrated in vacuo. The aqueous solution was extracted with ethyl acetate (2 × 50 mL) and evaporated to afford the desired carboxylic acid **13** (0.17 g, 89.9%)). LRMS (ESI⁻): 280.2 (M − H). ¹H NMR (CDCl₃ + DMSO-d_6) δ: 7.82 (d, J = 1.47 Hz), 7.78 (dd, J = 8.0, 1.47 Hz, 1H), 7.63 (t, J = 7.3, 8.42, 1H), 7.29 (s, 1H).

1-{3-[Amino(imino)methyl]phenyl}-N-[2′-(aminosulfonyl)[1,1′-biphenyl]-4-yl]-3-(trifluoromethyl)-1H-pyrazole-5-carboxamide, Trifluoroacetic Acid Salt (14a). To the pyrazole carboxylic acid **12** (0.35 g, 1.2 mmol) dissolved in methylene chloride (50 mL) was added oxalyl chloride (0.15 mL, 1.7 mmol) and 2 drops of DMF. The reaction was stirred for 2 h at room temperature and concentrated in vacuo. The residue was redissolved in methylene chloride (10 mL). 4′-Amino[1,1′-biphenyl]-2-*tert*-butylsulfonamide (0.38 g, 1.25 mmol) and N,N-dimethylaminopyridine (0.38 g, 3.1 mmol) were added, and the reaction was stirred at room temperature for 24 h. The reaction was concentrated and the residue quenched with HCl (3 N, 50 mL). The organics were extracted with ethyl acetate (2 × 100 mL), washed with saturated NaHCO₃ (50 mL) and brine (50 mL), and dried (magnesium sulfate). The crude product was purified via silica gel flash chromatography (hexanes/ethyl acetate, 1:1) to afford the desired coupled product 0.41 g (58%). LRMS (ESI⁺): 590 (M + Na). ¹H NMR (CDCl₃ + DMSO-d_6) δ: 9.88 (s, 1H), 8.18 (dd, J = 7.69, 1.47 Hz, 1H), 7.87 (d, J = 1.83 Hz, 1H), 7.79 (m,4H), 7.64 (m, 3H), 7.50 (m, 3H), 7.30 (d, J = 7.3 Hz, 1H), 3.67 (s, 1H), 1.02 (s, 9H). Following the Pinner amidine reaction described previously, the desired product **14a** was obtained (46%). LRMS (ESI⁺): 529.03 (M + H). ¹H NMR (DMSO-d_6) δ: 10.85 (s, 1H), 9.47 (s, 1.5H), 9.20 (s, 1.5H), 8.05 (s, 1H), 8.04 (dd, J = 7.69, 1.84 Hz, 1H), 7.96 (m, 2H), 7.82 (d, J = 7.69 Hz, 1H), 7.75 (s, 1H), 7.68 (d, J = 8.79 Hz, 2H), 7.62 (m, 2H), 7.39 (d, J = 8.43 Hz, 2H), 7.32 (sm, 3H). HRMS (C₂₄H₂₀F₃N₆O₃S): calcd 529.1270; found, 529.1267. HPLC purity >95%. Anal. calcd for C₂₄H₁₉-F₃N₆O₃S·1.2TFA·1.0H₂O; C, 46.40; H, 3.27; N, 12.30; found, C, 46.11; H,3.06; N, 12.05.

1-[3-(Aminomethyl)phenyl]-N-[2′-(aminosulfonyl)[1,1′-biphenyl]-4-yl]-3-methyl-1H-pyrazole-5-carboxamide, trifluoroacetic Acid Salt (17a). 1-(3-Cyanophenyl)-5-[[(2′-aminosulfonyl-[1,1′]-biphen-4-yl)aminocarbonyl]-3-methylpyrazole **13a** (0.19 g, 0.41 mmol) was dissolved in ethanol (20 mL). To this solution was added TFA (0.5 mL) and palladium on carbon (10%, 10 mg), and the mixture was hydrogenated on a Parr apparatus at 40 psi for 18 h. The mixture was filtered, concentrated, and purified by reverse phase HPLC to afford the title compound **17a** (17 mg, 9%). LRMS (ESI⁺): 462 (M + H). ¹H NMR (DMSO-d_6) δ: 10.66 (s, 1H), 8.22 (bd, 2H), 8.03 (dd, J = 1.47, 6.22 Hz, 1H), 7.70 (d, J = 8.79 Hz, 2H), 7.67 (m, 2H), 7.64 (m, 5H), 7.37 (d, J = 8.43 Hz, 2H), 7.32 (m, 2H), 6.93 (s, 1H), 4.13 (d, J = 4.03 Hz, 2H), 2.33 (s, 3H). HRMS (C₂₄H₂₄N₅O₃S): calcd 462.1599; found, 462.1589. HPLC purity >95%. Anal. calcd for C₂₄H₂₃N₅O₃S·1.0TFA·1.5H₂O; C, 51.82, H, 4.52, N, 11.62; found, C, 51.80, H, 4.35, N, 11.29.

1-[3-(Aminomethyl)phenyl]-N-[3-fluoro-2′-(methylsulfonyl)[1,1′-biphenyl]-4-yl]-3-(trifluoromethyl)-1H-pyrazole-5-carboxamide, Trifluoroacetic Acid Salt (17h). Prepared following the procedure for **17a**. LRMS (ESI⁺) 532 (M + H). ¹H NMR (DMSO-d_6) δ: 10.75 (s, 1H), 8.23 (m, 3H), 8.11 (dd, J = 7.69 and 1.46 Hz, 1H), 7.96 (dd, J = 6.96, 1.47 Hz, 1H), 7.81 (m, 8H), 7.26 (dd, J = 1.47 and 8.06 Hz, 1H), 4.16 (q, J = 5.49 Hz, 2H), 2.94 (s, 3H). HRMS (C₂₅H₂₁F₄N₄O₃S): calcd 533.1192; found, 533.1279. HPLC purity >95%. Anal. calcd for C₂₅H₂₀F₄N₄O₃S·1.1TFA; C, 49.65, H, 3.23, N, 8.52, found, C, 49.73, H, 2.98, N, 8.40.

1-[3-(Aminomethyl)phenyl]-N-[3-fluoro-2′-(methylsulfonyl)[1,1′-biphenyl]-4-yl]-3-(trifluoromethyl)-1H-pyrazole-5-carboxamide, Hydrochloride Salt (DPC423). Compound **17h** (0.47 g, 0.727 mmol) was dissolved in absolute methanol (30 mL). The mixture was cooled to 0 °C, and dry HCl gas was bubbled for 15 min. To this solution was added diethyl ether (400 mL) upon which a white solid precipitated. The solid

was collected and recrystallized from MeOH/EtOAc to afford 0.34 g (82.9%) of a colorless crystalline solid. mp: 288 °C. ¹H NMR (DMSO-d_6) δ: 10.83 (s, 1H), 8.44 (s, 2H), 8.11 (dd, J = 1.1, 7.7 Hz, 1H), 7.81 (m, 6H), 7.62 (m, 2H), 7.44 (dd, J = 1.1, 7.3 Hz, 1H), 7.41 (dd, J = 1.8, 11.4, 1H), 7.25 (dd, J = 1.5, 8.1 Hz, 1H), 4.13 (s, 2H), 2.94 (s, 3H). HRMS (C₂₅H₂₁F₄N₄O₃S): calcd 533.1192; found, 533.1282; HPLC purity > 95%; Anal. calcd for C₂₅H₂₁F₄N₄O₃S₁·1.0HCl; C, 52.77, H, 3.72, N, 9.85, Cl, 6.23; found, C, 52.86, H, 3.45, N, 9.74, Cl, 6.30.

References

(1) This work was partially presented: (a) Wexler, R. R. The design and synthesis of orally bioavailable noncovalent factor Xa inhibitors. 27th National Medicinal Chemistry Symposium, Kansas City, MO, June 13−17, 2000. (b) Pinto, D. J. P.; Orwat, M. J.; Wang, S.; Amparo, E.; Pruitt, J. R.; Rossi, K. A.; Alexander, R. S.; Fevig, J. M.; Cacciola, J.; Lam, P. Y. S.; Knabb, R. M.; Wong, P. C.; Wexler, R. R. The discovery of a novel pyrazole SN429, a highly potent inhibitor of coagulation factor Xa. *Abstracts of Papers*, 217th National Meeting of the American Chemical Society, Anaheim, CA, March 21−25, 1999; American Chemical Society: Washington, DC, **1999**; MEDI-006.

(2) (a) Hirsh, J.; Fuster, V. Guide to anticoagulant therapy. Part 2: Oral anticoagulants. *Circulation* **1994**, *89*, 1469−1480. (b) Hirsh, J. Oral anticoagulant drugs. *New Engl. J. Med.* **1991**, *324*, 1865−1875.

(3) Lefkovits, J.; Topol, E. J. Direct thrombin inhibitors in cardiovascular medicine. *Circulation* **1994**, *90*, 1522−1568.

(4) (a) Rihal, C. S.; Flather, M.; Hirsh, J.; Yusuf, S. Advances in antithrombotic drug therapy for coronary artery disease. *Eur. Heart J.* **1995**, *16*, 10−21. (b) Fareed, J.; Callas, D. D.; Hoppensteadt, D.; Jeske, W.; Walenga, J. M. Recent development in antithrombotic agents. *Exp. Opin. Invest. Drugs* **1995**, *4* (50), 389−412. (c) Hirsh, J. Use of Warfarin (Coumadin). *Heart Dis. Stroke* **1993**, *2*, 209−216. (d) Dalen, J. E.; Hirsh, J. Antithrombotic therapy. Introduction. *Chest* **1992**, *102*, 303S−304S.

(5) (a) Stein, P. D.; Grandison, D.; Hua, T. A. Therapeutic level of anticoagulation with warfarin in patients with mechanical prosthetic heart valves; review of literature and recommendations based on internal normalized ratio. *Postgrad. Med. J.* **1994**, *70* (suppl 1), S72−S83. (b) Hirsh, J.; Poller, L. The international normalized ratio. A guide to understanding and correcting its problems. *Arch. Int. Med.* **1994**, *154*, 282−288.

(6) (a) Berry, C. N.; Girardot, C.; Lecoffre, C.; Lunven, C. Effects of synthetic thrombin inhibitor argatroban on fibrin or clot-incorporated thrombin: comparison with heparin and recombinant hirudin. *Thromb. Haemostat.* **1994**, *72*, 381−386. (b) Kelly, A. G.; Marzee, W. M.; Krupski, W.; Bass, A.; Cadroy, Y.; Hanson. S. R.; Harker, L. A. Hirudin interruption of heparin-resistant arterial thrombus formation in baboons. *Blood* **1991**, *77*, 1006−1012.

(7) (a) Tapparelli, C.; Metternich, R.; Ehrhardt, C.; Cook, N. S. Synthetic low-Molecular weight thrombin inhibitors: molecular design and pharmacological profile. *Trends Pharmacol. Sci.* **1993**, *14*, 366−376. (b) Maffrand, J. P. Direct thrombin inhibitors. *Nov. Rev. Fr. Hematol.* **1992**, *34*, 405−419.

(8) (a) Rosenberg, J. S.; Beeler, D. L.; Rosenberg, R. D. Activation of human prothrombin by highly purified human factor V and FXa in presence of human antithrombin. *J. Biol. Chem.* **1995**, *250*, 1607−1617. (b) Davre, E. W.; Fujikawa, K.; Kisiel, W. The coagulation cascade: Initiation, maintenance and regulation. *Biochemistry* **1991**, *30*, 10363−10370. (c) Rosenberg, R. D.; Damus, P. S. Purification and mechanism of action of human antithrombin-heparin cofactor. *J. Biol. Chem.* **1973**, *248*, 6498−6505.

(9) Mann, K. G.; Nesheim, M. E.; Church, W. R.; Haley, P.; Krishnaswamy, S. Surface-dependent enzyme complexes. *Blood* **1990**, *76*, 1−16.

(10) (a) Fevig, J. M.; Wexler, R. R. (Doherty, A. M., Ed.) Anticoagu-
lants: Thrombin and Factor Xa inhibitors. *Annu. Rep. Med.
Chem.* **1999**, *34*, 81−100. (b) Sanderson, P. E. J. Small, non-
covalent serine protease inhibitors. *Med. Res. Rev.* **1999**, *19*,
179−197. (c) Hauptmann, J.; Sturzebecher, J. Synthetic inhibi-
tors of thrombin and factor Xa: from bench to bedside. *Thromb.
Res.* **1999**, *93*, 203−241. (d) Fareed, J.; Callas, D.; Hoppensteadt,
D. A.; Lewis, B. E.; Bick, R. L.; Walenga, J. M. Antithrombin
agents as anticoagulants and antithrombotics: implications in
drug development. *Semin. Hematol.* **1999**, *36* (1, Suppl. 1), 42−
56. (e) Kimball, S. D. Oral thrombin inhibitors: Challenges and
progress. *Handb. Exp. Pharmacol.* **1999**, *132* (Antithrombotics),
367−396. (f) Vacca J. P. (Bristol, J. A., Ed.) *Annu. Rep. Med.
Chem.* **1998**, *33*, 81−90.
(11) (a) Zhu, B.-Y.; Scarborough, R. M. Recent advances in inhibitors
of factor Xa in the prothrombinase complex. *Curr. Opin. Car-
diovasc., Pulm. Renal Invest. Drugs* **1999**, *1* (1), 63−87. (b) Al-
Obeidi, F.; Ostrem, J. A. Factor Xa inhibitors by classical and
combinatorial chemistry. *Drug Discovery Today* **1998**, *3* (5), 223−
231. (c) Scarborough R. M. Coagulation factor Xa: The pro-
thrombinase complex as an emerging therapeutic target for
small molecule inhibitors. *J. Enzymol. Inhib.* **1998**, *14*, 15−25.
(d) Hara, J.; Yokoyama, A.; Tanabe, K.; Ishihara, H.; Iwamoto,
M. DX-9065a an orally active specific inhibitor of factor Xa
inhibits thrombosis without affecting bleeding time in rats.
Thromb. Haemost. **1995**, *74*, 635−639. (e) Schaffer, J. A.;
Davidson, J. T.; Vlasuk, G. P.; Siegl, P. K. Antithrombotic
efficacy of recombinant tick anticoagulant peptide: a potent
inhibitor of coagulation factor Xa in a primate model of arterial
thrombosis. *Circulation* **1991**, *84*, 1741−1748.
(12) (a) Lynch, J. J.; Sitko, G. R.; Lehman, E. D.; Vlasuk, G. P.
Primary prevention of coronary arterial thrombosis with the
factor Xa inhibitor rTAP in a canine electrolytic injury model.
Thromb. Haemost. **1995**, *74*, 640−645. (b) Ramjit, D. R.; Sta-
bilito, D. R.; Lehman, I. I.; Lynch, J. J.; Vlasuk, G. P. Conjunctive
enhancement of enzymatic thrombolysis and prevention of
thrombotic reocclusion with the selective factor Xa inhibitor, Tick
anticoagulant peptide: Comparison to hirudin and heparin in
a canine model of acute coronary artery thrombosis. *Circulation*
1992, *85*, 805−815.
(13) a) Phillips, G.; Davey, D. D.; Eagen, K. A.; Koovakkat, S. K.;
Liang, A.; Ng, H. P.; Pinkerton, M.; Trinh, L.; Whitlow, M.;
Beatty, A. M.; Morrissey, M. M. Design, synthesis and activity
of 2,6-diphenoxypyridine-derived factor Xa inhibitors. *J. Med.
Chem.* **1999**, *42*, 1749−1756. (b) Galemmo, R. A., Jr.; Maduskuie,
T. P.; Dominguez, C.; Rossi, K. A.; Knabb, R. M.; Wexler, R. R.;
Stouten, P. F. W. The de novo design and synthesis of cyclic urea
inhibitors of factor Xa: initial SAR studies, *Bioorg. Med. Chem.
Lett.* **1998**, *8*, 2705−2710. (c) Maduskuie, T. P. Jr.; McNamara,
K. J.; Ru, Y.; Knabb, R. M.; Stouten, P. F. W. Rational design
and synthesis of novel potent Bis-phenylamidine carboxylate
factor Xa inhibitors. *J. Med. Chem.* **1998**, *41*, 53−62. (d) Quan,
M. L.; Pruitt, J. R.; Ellis, C. D.; Liauw, A. Y.; Galemmo, R. A.;
Stouten, P. F. W.; Wityak, J.; Knabb, R. M.; Thoolen, M. J.;
Wong, P. C.; Wexler, R. R. Design and synthesis of isoxazoline
derivatives as factor Xa inhibitors. *Bioorg. Med. Chem. Lett.*
1997, *7*, 2813−2818. (e) Sato, K.; Kawasaki, T.; Yaniuchi, Y.;
Hismichi, N.; Koshio, H.; Matsumoto, Y. YM-60828, a novel
factor Xa inhibitor: Separation of its antithrombotic effects from
its prolongation of bleeding time. *Eur. J. Pharmacol.* **1997**, *339*,
141−146. (f) Nagahara, T.; Yukoyama, Y.; Inamura, K.; Kataku-
ra, S.; Yamaguchi, H.; Hara, T.; Iwamoto, M. Design, synthesis
and biological activities of orally active coagulation factor Xa
inhibitors. *Eur. J. Med. Chem.* **1995**, *30*, 139. (g) Nagahara, T.;
Yukoyama, Y.; Inamura, K.; Hara, T.; Iwamoto, M. Dibasic
(amidinoaryl)propanoic acid derivatives as novel blood coagula-
tion factor Xa inhibitors. *J. Med. Chem.* **1994**, *37*, 1200−1207.
(h) Sturzebecher, J.; Markwardt, F.; Walsmann, P. Synthetic
inhibition of serine proteinases XXIII. Inhibition of factor Xa
by diamidines. *Thromb. Res.* **1980**, *17*, 545−548. (i) Sturze-
becher, J.; Markwardt, F.; Walsmann, P. Synthetic inhibitors
of serine proteinases XIV. Inhibition of factor Xa by derivatives
of benzamidines. *Thromb. Res.* **1976**, *9*, 637−646.
(14) (a) Quan, M. J.; Liauw, A. Y.; Ellis, C. D.; Pruitt, J. R.; Bostrom,
L. L.; Carini, D. J.; Huang, P. P.; Harrison, K.; Knabb, R. M.;
Thoolen, M. J.; Wong, P. C.; Wexler, R. R. Design and synthesis
of isoxazoline derivatives as factor Xa inhibitors. 1. *J. Med.
Chem.* **1999**, *42*, 2752−2759. (b) Quan, M. J.; Ellis, C. D.; Liauw,
A. Y.; Alexander R.; Knabb, R. M.; Lam G. N.; Wong, P. C.;
Wexler, R. R. Design and synthesis of isoxazoline derivatives
as factor Xa inhibitors. 2. *J. Med. Chem.* **1999**, *42*, 2760−2773.
(15) Pruitt, J. R.; Pinto, D. J.; Quan, M. L.; Estrella, M. J.; Bostrom,
L. L.; Knabb, R. M.; Wong, P. C.; Wexler, R. R. Isoxazolines and
isoxazoles as factor Xa inhibitors. *Bioorg. Med. Chem. Lett.* **2000**,
10 (8), 685−689.
(16) Jones, R. G.; Whitehead, C. W. Vic-Dicarboxylic acid derivatives
of pyrazole, isoxazole and pyrimidine. *J. Org. Chem.* **1955**, *20*,
1342−1347.
(17) Ashton, W. T.; Doss, G. A. A Regioselective route to 3-alkyl-1-
aryl-1H-pyrazole-5-carboxylates: Synthetic studies and struc-
tural assignments. *J. Heterocycl. Chem.* **1993**, *30*, 307−311.
(18) Basha, A.; Lipton, M.; Weinreb, S. M. *Tetrahedron Lett.* **1977**,
48, 4171−4174.
(19) Molecular models were compared using the Insight II program
developed by Molecular Simulations Inc. molecular modeling
program (version 97.2). For similar models, refer to ref 14.
Padmanabhan, K.; Padmanabhan, K. P.; Tulinsky, A.; Park, C.
H.; Bode, W.; Blankenship, D. T.; Cardin, A. D.; Kisiel, Structure
of human Des (1-45) factor Xa at 2.2 Ang. resolution W. *J. Mol.
Biol.* **1993**, *232* (3), 947−966.
(20) (a) Krishnaswamy, S.; Vlasuk, G. P.; Bergum, P. W. Assembly
of the prothrombinase complex enhances the inhibition of bovine
factor Xa by tick anticoagulant peptide. *Biochemistry* **1994**, *33*,
7897−7907. (b) Jordan, S. P.; Waxman, L.; Smith, D. E.; Vlasuk,
G. P. Tick anticoagulant peptide: Kinetic analysis of the
recombinant inhibitor with blood coagulation factor Xa. *Bio-
chemistry* **1990**, *29*, 11095−111000. (c) Waxman, L.; Smith, D.
E.; Arcuri, K. E.; Vlasuk, G. P. Tick anticoagulant peptide (TAP)
is a novel inhibitor of blood coagulation factor Xa. *Science* **1990**,
248, 593−596.
(21) (a) Brandstetter, H.; Kühne, A.; Bode, W.; Huber, R.; Von der
Saal, W.; Wirthensohn, K.; Engh, R. A. *J. Biol. Chem.* **1996**, *47*,
29988−29992. (b) Stubbs, M. T.; Structural Aspects of Factor
Xa Inhibition. *Curr. Pharm. Des.* **1996**, *2*, 543−552. (c) Stubbs,
M. T.; Huber R.; Bode, W. Crystal structures of factor Xa
inhibitors in complex with trypsin: structural grounds for
inhibition of factor Xa and selectivity against thrombin. *FEBS
Lett.* **1995**, *375*, 103−107.
(22) (a) Brandstetter, H.; Turk, D.; Hoeffken, H. W.; Grosse, D.;
Sturzebecher, J.; Martin, P. D.; Edwards, B. F.; Bode, W. Refined
2.3 Å X-ray crystal structure of bovine thrombin complexes
formed with the benzamidine and arginine-based thrombin
inhibitors NAPAP, 4-TAPAP and MQPA. A starting point for
improving antithrombotics. *J. Mol. Biol.* **1992**, *226*, 1085−1099.
(b) Turk, D.; Sturzebecher, J.; Bode, W. Geometry of binding of
the N-alpha-tosylated piperidides of m-amidino, p-amidino and
p-guanidino phenylalanine to thrombin and trypsin. X-ray
crystal structures of their trypsin complexes and modeling of
their thrombin complexes. *FEBS Lett.* **1991**, *287*, 133−138. (c)
Banner, D. W.; Hadvary, P. Crystallographic analysis at 3.0-A
resolution of the binding to human thrombin of four active site-
directed inhibitors. *J. Biol. Chem.* **1991**, *266*, 20085−20093. (d)
Bode, W.; Turk, D.; Sturzebecher J. Geometry of binding of the
benzamidine and arginine-based inhibitors N-alpha-(2-naphthyl-
sulphonyl-glycyl)-DL-p-amidinophenylalanyl-piperidine (NA-
PAP) and (2R,4R)-4-methyl-1-[N-alpha-(3-methyl-1,2,3,4-tet-
rahydro-8-quinolinesulphonyl)-L-arginyl]-2-piperidine carboxylic
acid (MQPA) tohuman alpha-thrombin. X-ray crystallographic
determination of the NAPAP-trypsin complex and modeling of
NAPAP-thrombin and MQPA-thrombin. *Eur. J. Biochem.* **1990**,
193, 175−182. (e) Matsuzaki, T.; Sasaki, C.; Okumura, C.;
Umeyama, H. J. X-ray analysis of a thrombin inhibitor-trypsin
complex. *Biochem. (Tokyo)* **1989**, *105*, 949−952.
(23) Bovine trypsin was purchased from Worthington (cat. #3707)
and used without further purification. Crystals were grown by
vapor diffusion using 20 μL hanging drops containing 10−30 mg/
mL β trypsin, 35 mM tris pH 7.5, 2.5 mM benzamidine, 100 mM
ammonium sulfate, and 6−12% W/V PEG 8000. The drops were
equilibrated at 5 °C over 50 mM tris pH 7.5, 200 mM ammonium
sulfate, and 12−24% W/V PEG 8000. Crystals appeared after
one week. Benzamidine was removed by letting the crystals soak
overnight in a stabilizing solution containing 50 mM tris pH 7.5,
200 mM ammonium sulfate, and 20% W/V PEG 8000. The
crystals were transferred to a solution containing 20 mM sodium
phosphate pH 7.5, 20% PEG 8000, and 0.1% glutaraldehyde for
30 min to cross-link. These crystals were then transferred to a
solution containing the inhibitor. The inhibitor solution was
prepared by first dissolving 1 mg of inhibitor in 5 μL of DMSO.
This was followed by a 40-fold dilution of the inhibitor/DMSO
solution into the first stabilizing solution. Data were collected
one week after inhibitor addition. A crystal of the trypsin-
inhibitor complex was mounted and sealed in a glass capillary.
An R-AXIS image plate detector was used for X-ray data
acquisition. A Rigaku RU-200 rotating anode X-ray generator
operating at 50 kV/100 mA equipped with a graphite monochro-
mator was used for data collection. The trypsin data were
collected at 40 °Celsius using an Enraf Nonius cooling device.
Data frames of 2° rotation about the spindle axis, φ, were
collected, with exposure times of 30 min/frame, for total angular
rotation ranges about φ of 90°. Data were processed using the
Raxis data processing software (Molecular Structure Corp.).
Crystals grew in space group *P*2₁2₁2₁ with the following unit
cell parameters: *a* = 54.8 Å, *b* = 59.6 Å, *c* = 66.8 Å. Data greater
than one σ were used in refinement and were 92% complete.
The XPLOR (Brünger, A. T.; Kuriyan, J.; Karplus, J. Crystal-
lographic R factor refinement by molecular dynamics. *Science*,

1987, *235*, 472−475) program was used for crystallographic refinement. Simulated annealing (at a maximum temperature of 3000 °C) was followed by B-factor refinement. The refined coordinates of trypsin (Krieger, M.; Kay, L. M.; Stroud, R. M. Structure and specific binding of trypsin: comparison of inhibited derivatives and a model for substrate binding. *J. Mol. Biol.* **1974**, *83*, 209−230) were used to calculate the initial phases for the enzyme−inhibitor structure. The inhibitor was built with the program QUANTA (Molecular Simulations Inc.). No major adjustments to the protein model were needed during the course of the refinements. The final crystallographic *R*-factor was 19.2%.

(24) Kiely, S.; John, J. S. The synthesis of Methyl 1-Aryl-2-pyrrole-carboxylates. *J. Heterocycl. Chem.* **1987**, *24*, 1137−1139.

(25) Kettner, C.; Mersinger, L.; Knabb, R. The selective inhibition of thrombin by peptides of boroarginine. *J. Biol. Chem.* **1990**, *265* (30), 18289−18297.

(26) Wong, P. C.; Quan, M. L.; Crain, E. J.; Watson, C. A.; Wexler, R. R.; Knabb, R. M. Nonpeptide Factor Xa Inhibitors I. Studies with SF303 and SK549, a new class of potent antithrombotics. *J. Pharmacol. Exp. Ther.* **2000**, *292*, 351−357.

(27) Hilgers, A. R.; Conradi, R. A.; Burton, S. Caco-2 cell monolayers as a model for drug transport across the intestinal mucosa. *Pharm. Res.* **1990**, *7*, 902−910.

(28) Gibaldi, M.; Perrier, D. *Pharamcokinetics*, 2nd ed.; Marcel Dekker: New York, 1982.

(29) Kallikrein, although essential for clotting of plasma in vitro, the in vivo significance of this hemostatic deficiency is not considered to be important, as patients with this abnomality do not require replacement therapy following hemostatic challenge from trauma or surgery. Mann, K. G.; Lorand, L. Introduction: Blood coagulation. *Methods Enzymol.* **1993**, *222*, 1−10.

(30) It also appears that measuring anti-fXa activity is a sensitive method for assessing fXa inhibitors ex vivo. The APTT and PT values for factor Xa inhibitors are not sensitive enough to monitor the antithrombotic effect of factor Xa inhibitors. Wong, P. C.; Crain, E. J.; Knabb, R. M.; Meade, R. P.; Quan, M. L.; Watson, C. A.; Wexler, R. R.; right, M. R.; Slee, A. M. Nonpeptide factor Xa inhibitors II. Antithrombotic evaluation in a rabbit model of electrically induced carotid artery thrombosis. *J. Pharmacol. Exp. Ther.* **2000**, *295*, 212−218.

(31) Wong, P. C.; Crain, E. J.; Watson, C. A.; Pinto, D. J.; Wexler, R. R.; Wright, M. R.; Knabb, R. M. Antithrombotic effects of DPC 423, a potent and orally active nonpeptide factor Xa inhibitor, in rabbit models of thrombosis. *Circulation* **2000**, *102* (18, Supp. II), 130.